VOLUME 29 · NUMBER 11 · APRIL 10 2011

JOURNAL OF CLINICAL ONCOLOGY

ORIGINAL REPORT

Integrative Genomic Analysis of Medulloblastoma Identifies a Molecular Subgroup That Drives Poor Clinical Outcome

Yoon-Jae Cho, Aviad Tsherniak, Pablo Tamayo, Sandro Santagata, Azra Ligon, Heidi Greulich, Rameen Berhoukim, Vladimir Amani, Liliana Goumnerova, Charles G. Eberhart, Ching C. Lau, James M. Olson, Richard J. Gilbertson, Amar Gajjar, Olivier Delattre, Marcel Kool, Keith Ligon, Matthew Meyerson, Jill P. Mesirov, and Scott L. Pomeroy

See accompanying editorial on page 1395 and articles on pages 1400, 1408, and 1415

From the Children's Hospital Boston; Harvard Medical School; Brigham and Women's Hospital; and Dana-Farber Cancer Institute, Boston; and Broad Institute of Massachusetts Institute of Technology and Harvard, Cambridge, MA; Johns Hopkins University Medical Center, Baltimore, MD; Texas Children's Cancer Center, Baylor College of Medicine, Houston, TX; Fred Hutchinson Cancer Research Center, University of Washington, Seattle, WA; St Jude Children's Research Hospital, Memphis, TN; Laboratoire de Génétique et Biologie des Cancers, Paris, France; and Academic Medical Center, Amsterdam, the Netherlands.

Submitted February 5, 2010; accepted September 2, 2010; published online ahead of print at www.jco.org on November 22, 2010.

Supported by Grants No. NIH-R01-109467, NIH-R33-CA97556-01, NIH-6R01-CA-121941-04, NIH-R01-GM074024, NIH-P50-CA112962, and NIH-R01-NS055089.

Authors' disclosures of potential conflicts of interest and author contributions are found at the end of this article.

Corresponding author: Scott L. Pomeroy, MD, PhD, Children's Hospital, 300 Longwood Ave, Boston, MA 02115; e-mail: scott.pomeroy@childrens.harvard.edu.

0732-183X/11/2911-1424/$20.00

DOI: 10.1200/JCO.2010.28.5148

ABSTRACT

Purpose
Medulloblastomas are heterogeneous tumors that collectively represent the most common malignant brain tumor in children. To understand the molecular characteristics underlying their heterogeneity and to identify whether such characteristics represent risk factors for patients with this disease, we performed an integrated genomic analysis of a large series of primary tumors.

Patients and Methods
We profiled the mRNA transcriptome of 194 medulloblastomas and performed high-density single nucleotide polymorphism array and miRNA analysis on 115 and 98 of these, respectively. Non-negative matrix factorization–based clustering of mRNA expression data was used to identify molecular subgroups of medulloblastoma; DNA copy number, miRNA profiles, and clinical outcomes were analyzed for each. We additionally validated our findings in three previously published independent medulloblastoma data sets.

Results
Identified are six molecular subgroups of medulloblastoma, each with a unique combination of numerical and structural chromosomal aberrations that globally influence mRNA and miRNA expression. We reveal the relative contribution of each subgroup to clinical outcome as a whole and show that a previously unidentified molecular subgroup, characterized genetically by *c-MYC* copy number gains and transcriptionally by enrichment of photoreceptor pathways and increased miR-183~96~182 expression, is associated with significantly lower rates of event-free and overall survivals.

Conclusion
Our results detail the complex genomic heterogeneity of medulloblastomas and identify a previously unrecognized molecular subgroup with poor clinical outcome for which more effective therapeutic strategies should be developed.

J Clin Oncol 29:1424-1430. © 2010 by American Society of Clinical Oncology

INTRODUCTION

Advancements in genome scale technologies have led to an evolving molecular classification of me dulloblastomas. Previous gene expression studies have suggested up to five molecular subtypes of this disease,[1-4] which include a subgroup with Sonic Hedgehog (SHH) pathway activation[1,5]; another characterized by β-catenin mutations and monosomy chromosome 6[4,6,7]; and others expressing neuronal differentiation markers, photoreceptor transcriptional markers, or both.[3]

Numerous genetic alterations have also been reported but have not been extensively detailed for the various molecular subgroups of medulloblastoma.[3,8-10] Similarly, miRNA studies have revealed their differential expression in medulloblastomas but have largely focused on the SHH pathway–activated subgroup without appreciating the heterogeneity reported at the mRNA level.[11-14]

Here, we present a genomic classification of medulloblastoma that is based on an analysis of 194 tumor samples. We identify distinct molecular subgroups of medulloblastoma with unique combinations of copy number alterations that globally influence mRNA and miRNA expression. We correlate clinical behavior of medulloblastomas in the context of these molecular subgroups and reveal a newly identified molecular subgroup with a particularly aggressive course. We validate our findings in three independently published data sets and, in a separate study, integrate our knowledge of molecular subtypes into a novel outcome prediction model.[14b]

PATIENTS AND METHODS

Biologic Samples

Tumors were serially accrued from Children's Oncology Group (COG) (ACNS02B3; n = 89; 2004 to 2007), Children's Hospital Boston (n = 55; 1996 to 2007), University of Washington (n = 27; 2001 to 2005), Texas Children's Hospital (n = 24; 2000 to 2004), and Johns Hopkins Medical Center (n = 10; 2000 to 2001). Normal cerebellum (n = 11) was obtained from University of Washington and the Eunice Kennedy Shriver National Institute of Child Health and Human Development (NICHD) Brain and Tissue Bank for Developmental Disorders, University of Maryland, Baltimore, MD. All samples were collected with approval from respective institutional review boards, and informed consent and/or assent was obtained from all patients or their parents.

Central histopathologic review was performed on patients from Children's Hospital Boston and COG. For samples obtained from University of Washington, Johns Hopkins, and Texas Children's, hematoxylin and eosin was not available; therefore, histopathology reports provided by the contributing institutions were reviewed.

Gene Expression, SNP Array, and miRNA Data

DNA and total RNAs were extracted as described in the Appendix (online online). Gene expression data were generated by using Affymetrix_HT-HG-U133A chips (Affymetrix, Santa Clara, CA). Microarray data from Kool et al,[3] Fattet et al,[7] and Thompson et al[4] were obtained from the Gene Expression Omnibus (GSE10327 and GSE12992) and from http://www.stjuderesearch.org/data/medulloblastoma/, respectively. Copy number data were generated from Affymetrix_250K_Sty and Affymetrix_6.0 arrays (Affymetrix). miRNA profiling was performed as previously described.[15,16]

Computational Methods

Detailed methods are provided in the Appendix (online only). Briefly, non-negative matrix factorization (NMF)[2]; silhouette width analysis[17,18]; gene set enrichment analysis (GSEA)[19,20]; genomic identification of significant targets in cancer (GISTIC) analysis[21,22]; and metagene projection[23] were performed as previously described.

Immunohistochemistry and Fluorescent In Situ Hybridization

Anti-CRX and GRM8 antibodies were obtained from Santa Cruz Biotechnology (Santa Cruz, CA) and Sigma-Aldrich (St Louis, MO), respectively. Probes for *c-MYC* and *MYCN* were obtained from Abbott Molecular. (Abbott Park, IL). *GLI2* BAC clones were obtained from CHORI (http://www.chori.org). Immunohistochemistry and fluorescent in situ hybridization (FISH) were performed on formalin-fixed, paraffin-embedded samples as previously described[24,25] (Appendix, online only).

Survival Analysis

Kaplan-Meier curves and log-rank statistics were generated by using GraphPad Prism (GraphPad Software, La Jolla, CA). Clinical annotations are provided in the Appendix (online only).

RESULTS

Unsupervised Clustering of mRNA Expression Data Identifies Six Medulloblastoma Subgroups

To identify molecular subtypes of medulloblastoma, we utilized an unsupervised clustering algorithm that was based on NMF.[2] NMF identifies metagenes, or aggregate patterns of gene expression, which are then used to determine the most stable clustering by calculating a cophenetic coefficient for each number of clusters. When applied to our gene expression microarray data consisting of 194 primary medulloblastomas and, for comparison, nine atypical teratoid/rhabdoid tumors (ATRTs), the optimal number of clusters in our data set is k = 7. These represent six medulloblastoma subgroups (designated c1 through c6) plus one ATRT subgroup (Fig 1A).

Silhouette width analysis[17] was performed to assess the similarity of each sample to its assigned subgroup compared with samples from other subgroups (Fig 1B). The average silhouette width for NMF subgroups was 0.62 (range, 0.4 to 0.85), suggesting samples within each subgroup are highly coherent (Fig 1B). The c2 and c4 subgroups displayed the lowest overall silhouette scores; at the gene expression level, significant overlap was seen between these subgroups (Fig 1C).

Functional Annotation of Medulloblastoma Subgroups

To identify biologic pathways associated with each NMF subgroup, we performed gene set enrichment analysis (GSEA)[19] with 2,163 annotated pathways. The c1 subgroup shows marked enrichment of *MYC* and related translational/ribosomal signatures. Also enriched are photoreceptor transcriptional programs, and expression of GABRA5, features prominent in c5 as well (Data Supplement). A pairwise GSEA between c1 and c5, however, substantiates the marked upregulation of MYC-related signatures as specific to c1 (Data Supplement).

c2 and c4 are characterized by neuronal differentiation markers, including increased expression of the metabotropic glutamatergic receptors GRM1 and GRM8 (Data Supplement). Despite considerable overlap between these subgroups, a pairwise GSEA revealed enrichment of gene sets related to tumor necrosis factor (TNF) -α/interferon (IFN) -β/nuclear factor-κB in c2, whereas signatures related to both MYC and neuronal development were enriched in c4 (Data Supplement).

Although c4 tumors predominantly express neuronal/glutamatergic signatures, they also express GABRA5 and the photoreceptor transcriptional program to some degree (Data Supplement). To investigate whether concomitant expression of both signatures represented distinct subclonal populations within the tumor, we performed immunostaining for CRX and GRM8, surrogate markers for the photoreceptor/GABAergic and neuronal/glutamatergic signatures, respectively. We identify nests of CRX-immunopositive cells that were distinct from GRM8-immunopositive cells, confirming the presence of subpopulations within c4 tumors and explaining their mixed gene expression signature (Data Supplement).

The c3 subgroup shows enrichment of gene sets associated with SHH signaling, as observed previously.[1] c6 was enriched with TGF-β, WNT/β-catenin, and epithelial mesenchymal transition (EMT) gene sets, consistent with previous reports[3,7] (Data Supplement).

Unique Combinations of Copy Number Alterations Define Each Molecular Subgroup

GISTIC analysis on our full cohort identified several genetic lesions that have been previously reported (Data Supplement).[8,10,21,26] To assess subgroup-specific copy number alterations and to evaluate their intersubgroup significance, we performed GISTIC analysis on NMF subgroups individually (Figs 2A and 2B; Data Supplement). As previously reported,[4,7,27] a strong correlation of monosomy chromosome 6 with the c6/WNT subgroup was observed (nine of nine; $P < .001$; Figs 2A and 2B).

We found *c-MYC* copy number gain exclusively in c1 (13 of 18; $P < .001$; Fig 2B; Data Supplement) along with frequent broad gains of 1q (12 of 18; $P = .0099$; Fig 2B; Data Supplement). Several *c-MYC* gains appeared focal and high level, which was suggestive of amplifications. Thus, we performed FISH for *c-MYC* and *MYCN* to confirm focal amplification of *c-MYC* in several c1 tumors and, less commonly, focal *MYCN* amplification in the rare samples without *c-MYC* gains

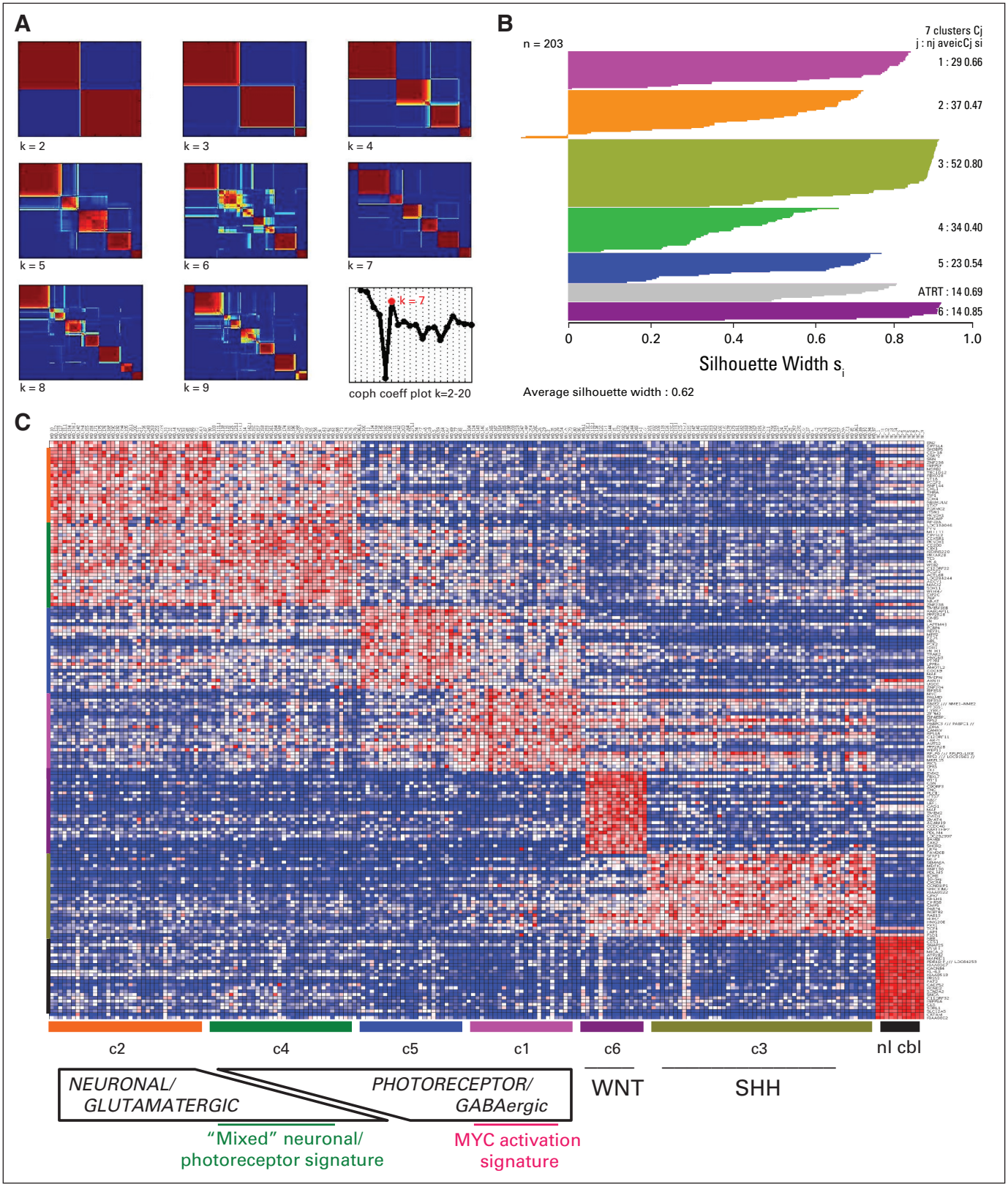

Fig 1. (A) Non-negative matrix factorization consensus clustering of mRNA expression array data from 194 primary medulloblastomas and nine atypical teratoid/rhabdoid tumors (ATRTs) reveals seven (k = 7) stable subgroups (six medulloblastoma subgroups, c1 through c6, plus an additional ATRT subgroup). (B) Silhouette widths indicate a strong similarity of samples to others within their subgroup relative to samples from other subgroups. (C) Heat map of the top 25 upregulated genes for each subgroup shows significant overlap between the c2 and c4 subgroups, which are characterized by enrichment of neuronal/glutamatergic signatures, and overlap to a lesser extent between c1 and c5 subgroups, which both have enrichment of photoreceptor transcriptional signatures; normal cerebellum samples are included to assess for the degree of stromal contamination. coph coeff, cophenetic coefficient; WNT, *Wingless* signaling pathway; SHH, *Sonic Hedgehog* signaling pathway.

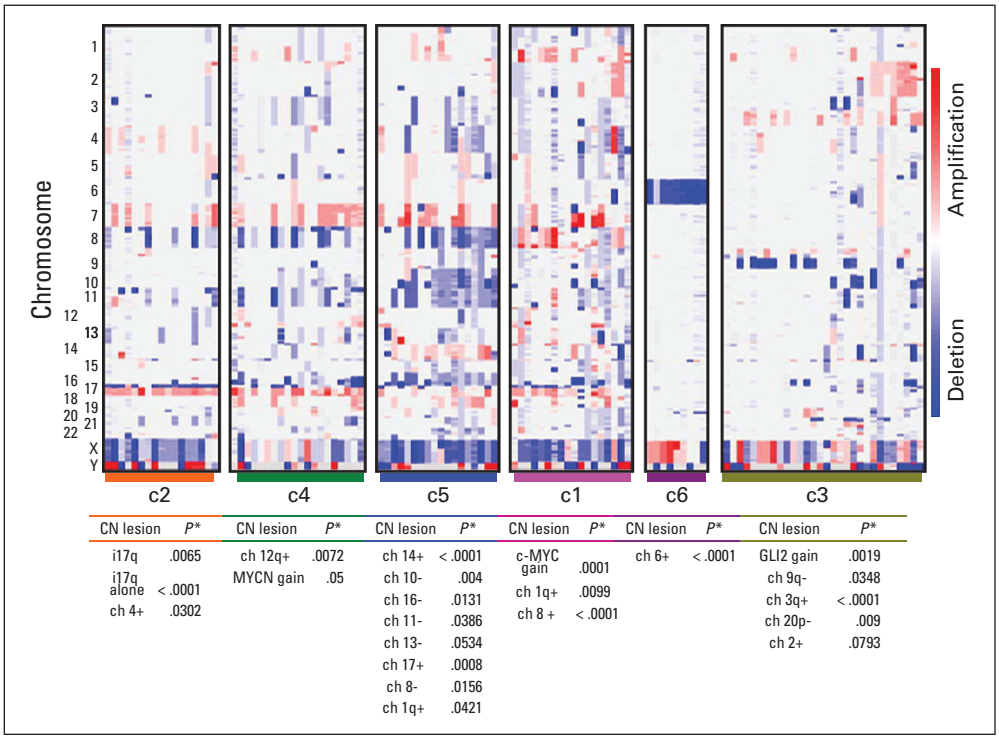

Fig 2. Copy number (CN) profiles of samples arranged by non-negative matrix factorization subgroup reveals statistically significant CN alterations associated with each. Detailed files of significant CN lesions within each subgroup, as determined by genomic identification of significant targets in cancer (GISTIC) analysis, are provided in the Data Supplement. ch, chromosome.

(Data Supplement). The one sample without *c-MYC* or *MYCN* copy number gains on SNP analysis had no evidence for subclonal amplification by FISH but had polysomy of chromosome 2, on which the *MYCN* locus resides.

Given the similarities between c1 and c5, we also performed FISH for *c-MYC* and *MYCN* on c5 tumors. Within the limits of this technique, we found no evidence of *c-MYC* amplifications, even subclonally. However, c5 tumors had numerous other copy number alterations, which were predominantly arm-level or whole-chromosome changes. The notable exception was focal *PTEN* and/or 10q loss (14 of 18; $P = .004$). Gain of 14 (11 of 18; $P < .001$), loss of 16 or 16q (17 of 18; $P = .0131$), and broad loss of 11 (13 of 18; $P = .0386$) were common (Figs 2A and 2B; Data Supplement). Isochromosome 17q (i17q) was notably underrepresented in c5 (five of 18) compared with c1 (11 of 18), c2 (15 of 17; $P = .0065$), and c4 (13 of 20); however, numerical gain of 17 (six of 18; $P = .0008$) was noted in c5. Neither c3 nor c6 had evidence for chromosome 17 alterations (Figs 2A and 2B; Data Supplement).

Differences between c2 and c4 become more apparent at the DNA level when compared with gene expression. In particular, c2 tumors had fewer genetic lesions than c4 tumors (Data Supplement). Core c2 tumors, as defined by the samples with the highest silhouette scores (Fig 1B), often had no more than an i17q ($P < .001$) and, occasionally, gain of chromosome 4 ($P = .0302$; Figs 2A and 2B; Data Supplement). Specific to c4 was gain of 12q (seven of 20; $P = .0072$). *MYCN* gain, often focal and high level, was also seen in 45% (nine of 20; $P = .05$) of c4 tumors, whereas low-level *c-MYC* gain was observed in 25% of the c4 subgroup (five of 20). Additional copy number alterations shared by other subgroups, such as gain of 7 and 18 and deletions of 8, 11, and 16q, were displayed by c4 tumors (Figs 2A and 2B; Data Supplement).

Notable genetic heterogeneity was observed in c3 tumors. Broad loss of 9q (13 of 30; $P = .0348$) and 20p (five of 30; $P = .009$) and gains of 3q (12 of 30; $P < .001$) were specific for this subgroup (Figs 2A and 2B; Data Supplement). Loss of 10q (seven of 30) and 16q (10 of 30) were frequent features of c3 that were also seen in other subgroups. Loss of 9q and 10q appeared to be mutually exclusive except in one sample. Both broad and focal gains were noted on chromosome 2 ($P = .0783$). In particular, focal gains of *GLI2* (five of 30; $P = .0019$), *MYCN* (three of 30), or—interestingly—both (two of 30) were observed (Data Supplement). FISH analysis for *GLI2* and *MYCN* confirmed their high-level gains in a subset of SHH-activated medulloblastomas (Data Supplement). We obtained analyzable FISH results on 19 c3/SHH tumors. We identified one sample with high-level *MYCN* amplification, one with focal *GLI2* amplification (plus polysomy for chromosome 2), and several with polysomy for chromosome 2 ($n = 8$). We did not find evidence for subclonal amplification of either *GLI2* or *MYCN* but did detect samples with subclonal (< 5% nuclei) polysomy for chromosome 2.

To assess the influence of DNA copy number alterations on gene expression, we performed GSEA on each NMF subgroup by using sets of genes that were based on their physical chromosomal location (ie, positional). We observed statistically significant gene expression changes concordant with chromosomal gains and losses identified in our subgroup-specific GISTIC analyses (Data Supplement). However, in c3/SHH tumors, a correlation between *GLI2* copy number gain and *GLI2* mRNA expression was not observed (Data Supplement).

Medulloblastoma Subgroups Have Distinct miRNA Profiles

As previously reported,[13,14] the miR-17~92 cluster is upregulated across medulloblastoma samples relative to normal cerebellum (Appendix Fig A1, online only; Data Supplement). The most robust expression of these miRNAs was noted in c1, c3, c5, and c6; lower levels of expression were noted in c2 and c4 (Fig 3). miR-21, a known oncomir,[28] was also upregulated across all tumors relative to normal

cerebellum (Data Supplement). Conversely, several miRNAs were highly expressed in normal cerebellum relative to primary medulloblastomas. c2 and c4 tumors appeared to have the most overlap with normal cerebellum miRNA expression consistent with the differentiated neuronal phenotype suggested by GSEA.

The miR-183∼96∼182 cluster is specific for medulloblastomas expressing photoreceptor transcriptional genes (c1, c5 and c4; $P < .001$), whereas miR-592 expression is observed primarily in c2 and c4 ($P < .001$). Thus, c4 tumors express both miR-592 and miR-183∼96∼182 ($P < .001$), which additionally corroborates the mixed subpopulations in these tumors (Data Supplement).

Finally, downregulation of miR-135a/b, miR-338, miR-124, and miR-138 and upregulation of miR-199b, miR-378, miR-28, miR-95 and miR-625 were noted in c3 tumors (Data Supplement). c6 tumors are distinctive in their marked upregulation of the miR-23∼27∼24 cluster (Fig A1; $P < .001$).

Demographic Characteristics of Molecular Subgroups

The general characteristics of our study population were consistent with those previously reported (Table 1).[29,30] A male predominance of 1.5 to 1 was noted for the full cohort and was largely driven by the c1 subgroup, which had a 3.8-to-1 male-to-female ratio. The median age for the cohort was 6.5 years. However, age distribution varied across subgroups; the c3/SHH subgroup contained the highest percentage of patients younger than 3 years of age (34%; $P = .0142$) and all patients older than 25 years of age (n = 4).

Nodular/desmoplastic histology was associated with c3 ($P < .001$), and large cell or anaplastic (LC/A) histologies were noted in all NMF subgroups. However, c5 and c1 had the highest percentages of LC/A (33.33% and 23%, respectively; $P = .0518$ and .2404, respectively). Interestingly, all patients with LC/A histology in the c3/SHH subgroup were older than 7 years of age, whereas patients with LC/A tumors in c5 were all younger than 7 years of age.

Aggressive Clinical Behavior Was Associated With c1 Subgroup

We analyzed event-free survival (EFS) and overall survival (OS) for 115 and 112 patients in our cohort, respectively. To minimize treatment heterogeneity, we excluded patients younger than 3 years of age (n = 16) and confirmed that all patients older than 3 years of age received treatment with radiation and chemotherapy. Individuals who died as a result of reasons other than primary disease (n = 3) were excluded.

Kaplan-Meier analysis revealed that poor clinical outcome was driven by c1 tumors ($P = .0514$ and .0105 for EFS and OS, respectively; Table 1; Appendix Fig A2A, online only). Patients with c3/SHH tumors also had relatively poor prognoses. Indeed, c1 and c3, together, were responsible for the majority of relapses and death caused by medulloblastoma as a whole. Intermediate rates of

Table 1. Clinicohistologic Characteristics of Individual NMF Subgroups and of the Overall Study Cohort

Variable	NMF Subgroup						Overall (N = 189)
	c1: MYC (n = 29)	c2: Neuronal (n = 37)	c3: SHH (n = 52)	c4: Mixed (n = 34)	c5: Photoreceptor (n = 23)	c6: WNT (n = 14)	
% of overall patients	15.34	19.58	27.51	17.99	12.17	7.40	
Sex, No.							
Male	23	25	25	21	16	3	113
Female	6	12	27	13	7	10	75
Male-to-female ratio	3.83	2.08	0.93	1.61	2.29	0.3	1.51
Age, months							
Median	64	103	67	84	64	96	79
Range	7-178	48-227	11-527	12-264	12-144	48-159	7-527
Age group by years, %							
< 3	25	0	34*	14.71	21.74	0	18.09
3-7	42.86	37.14	22	41.48	56.52	30.77	35.64
7-12	17.86	51.43	20	23.53	21.74	53.85	28.19
12-18	14.29	8.57	16	17.65	0	15.38	12.23
18-25	0	2.86	2	2.94	0	0	1.60
> 25	0	0	6	0	0	0	1.60
Histologic subtype, %							
Classic	73	85.7	51	79.4	61.9	85.71	71
Nodular/desmoplastic	4	11.4	38.3*	8.8	4.76	0	15.3
Large cell/anaplastic	23	2.86	10.6	11.8	33.33	7.1	13.6
M+ disease							
No.	7	4	8	4	0	1	24
No. evaluated	25	30	42	31	21	12	163
%	28	13.33	18.18	12.90	0	8.33	14.72
Relapse-free survival, %†	21.01	51.94	57.65	76.35	68.38	81.82	60.56
Overall survival, %†	21.01‡	87.67	64.99	95	74.07	90.91	73.57

Abbreviations: NMF, non-negative matrix factorization; SHH, Sonic Hedgehog.
*Statistically significant *P* value (< .05) for association of subgroup *v* all other subgroups.
†Kaplan-Meier adjusted 6-year survival (EFS and OS) for patients greater than 36 months of age.
‡Statistically significant difference between survival curves for subgroup patients *v* all other patients (log-rank test).

EFS and OS were seen in c5 and c2. Patients with c6 tumors appeared to have good clinical outcome, consistent with previous reports (Data Supplement).[7,27]

To investigate whether our results were biased by the exclusion of patients younger than 3 years of age, we analyzed survival from the whole patient cohort without filtering for age, and we also analyzed the age group younger than 3 years old independently (Data Supplement). Although the small number of patients in the age group younger than 3 years old limited statistical significance, patients with c1 tumors still fared poorly irrespective of age, whereas patients with c4 tumors in the age group younger than 3 years old fared worse relative to the older age groups (Data Supplement). Patients with c3 tumors appeared to have equivalent survival trends in both age groups.

Validation of Findings in Three Independent Medulloblastoma Data Sets

We analyzed data sets published by Thompson et al,[4] Kool et al,[3] and Fattet et al[7] by building a classifier that was based on metagene projection[23] to assign samples from each data set to the NMF subgroups identified in this study (Data Supplement). A heatmap of the top marker genes for each subgroup again revealed overlap between c2 and c4 (Figs A3A and A5B, online only). GSEA of positional gene sets in these subgroups confirmed copy number–driven gene expression changes similar to the GISTIC and positional GSEA results obtained on our data set (Data Supplement). Importantly, the equivalent c1 subgroups showed enrichment of genes at the *c-MYC* locus (8q24). Accordingly, genes along chromosome 14 were enriched in the c5 subgroup, whereas genes at the *PTEN* locus (10q23) were enriched in nonc5 tumors relative to c5, suggesting gain of chromosome 14 and loss of chromosome 10/10q, respectively (Data Supplement).

In a separate analysis, we performed consensus NMF clustering on the validation data sets by using parameters that identified the six subgroups in our data set. In a combined data set of Kool et al[3] and Fattet et al[7], NMF clustering identified six subgroups similar to those in our data set. In the data set of Thompson et al[4], however, eight subgroups were identified because of splits in the c3/SHH and c6/WNT subgroups. Silhouette analysis revealed one of the additional c6/WNT subgroups had a low silhouette width (S_i, 0.03) and that the extra c3/SHH subgroup had a notable degree of stromal contamination signature that was based on the signature from our normal cerebellum samples.

Validation of Poor Survival Associated With c1 Subgroup Tumors

Survival data from a combined total of 102 patients from the three validation cohorts was analyzed. Again, patients younger than 3 years of age (n = 21) and patients older than 3 years of age who received no radiation therapy (n = 8) were analyzed independently.

Kaplan-Meier analysis confirmed that poor clinical outcome was associated with c1 tumors ($P = .0019$; Appendix Fig A3C, online only). Statistically significant differences in survival curves were not achieved for other NMF subgroups; however, c5 and c6 appeared to have the best overall survival ($P = .1654$ and .1433, respectively; Fig A3C).

In patients younger than 3 years of age (and in patients older than 3 years of age who received no radiotherapy), c1 tumors were again associated with decreased survival (Data Supplement); however, the size of these cohorts limited their statistical significance. Younger patients with c5 tumors also fared worse relative to their older counterparts (Data Supplement).

DISCUSSION

Our integrated genomic analysis identified six distinct subgroups of medulloblastoma. However, given the similarities between c1 and c5 subgroups and the c2 and c4 subgroups, one could imagine four broad medulloblastoma subgroups: photoreceptor/GABAergic (composed of c1 and c5), neuronal/glutamatergic (composed of c2 and c4), SHH, and WNT/β-catenin. Yet, key differences exist between these subgroups (Data Supplement). As first described by Kool et al,[3] there are several medulloblastomas that have both neuronal/glutamatergic and photoreceptor/GABAergic features. We have provided evidence that this mixed signature, seen in our c4 subgroup, results from distinct subclonal populations within these tumor (Data Supplement). This also explains overlaps in our miRNA data, in which tumors expressed either miR-592 alone (c2), miR-183~96~182 alone (c1, c5), or both miR-592 and miR-183~96~182 together (c4; Data Supplement). Interestingly, miR-592 is physically located within an intron of the *GRM8* gene, which suggests a common transcriptional regulation; conversely, miRNA-96~182~183 has been implicated in retinal development and stem-cell maintenance.[31-33]

The distinction between c1 and c5 is less subtle, and our findings clearly implicate *MYC* activation, predominantly via genomic amplification, as highly specific for c1 tumors. From a clinical standpoint, distinguishing c1 from c5 is critically important, as patients with c1 tumors in our cohort and three independent cohorts had poor survival (Figs A2A and A3C). Whether this warrants more aggressive up-front therapy for patients with c1 tumors will need to be determined. Nonetheless, our results emphasize that, if treatment stratification is based on four molecular subgroups rather than six, and if patients with c1 and c5 tumors are treated similarly, an unacceptable number of patients would be overtreated on the basis of an errant assumption that c1 and c5 tumors share the same clinical behavior.

Other than the c1 subgroup (and perhaps c6), however, there are no other strong associations with outcome and NMF subgroup. We also acknowledge that our results merely associate clinical outcome with molecular subgroups rather than actively predict outcome for individual patients. Therefore, in a concurrent study, we describe an outcome prediction model that incorporates molecular subtypes into risk stratification by identifying factors that influence outcome within each subgroup.[14b]

Finally, within the c3/SHH subgroup, we observe notable genetic heterogeneity, which has tremendous implications on the efficacy of targeted therapies currently entering clinical trials (eg, smoothened inhibitors). In particular, *MYCN* and *GLI2*, both downstream mediators of the SHH signaling pathway, are amplified in some c3 tumors. Given that smoothened inhibitors target the SHH pathway upstream of GLI2 and MYCN, one might predict *GLI2*- or *MYCN*-amplified tumors to be refractory to these therapies.[34,35] Thus, our results emphasize the importance of having genomic data to inform clinical trials, either up front or in post hoc analyses.

AUTHORS' DISCLOSURES OF POTENTIAL CONFLICTS OF INTEREST

The author(s) indicated no potential conflicts of interest.

AUTHOR CONTRIBUTIONS

Conception and design: Yoon-Jae Cho, Pablo Tamayo, Jill P. Mesirov, Scott L. Pomeroy
Financial support: Matthew Meyerson, Jill P. Mesirov, Scott L. Pomeroy
Provision of study materials or patients: Yoon-Jae Cho, Liliana Goumnerova, Charles G. Eberhart, Ching C. Lau, James M. Olson, Richard J. Gilbertson, Amar Gajjar, Marcel Kool, Keith Ligon, Scott L. Pomeroy
Collection and assembly of data: Yoon-Jae Cho, Aviad Tsherniak, Pablo Tamayo, Sandro Santagata, Azra Ligon, Heidi Greulich, Rameen Berhoukim, Vladimir Amani, Liliana Goumnerova, Charles G. Eberhart, Ching C. Lau, James M. Olson, Richard J. Gilbertson, Amar Gajjar, Olivier Delattre, Keith Ligon, Matthew Meyerson, Jill P. Mesirov, Scott L. Pomeroy
Data analysis and interpretation: Yoon-Jae Cho, Aviad Tsherniak, Pablo Tamayo, Sandro Santagata, Azra Ligon, Heidi Greulich, Rameen Berhoukim, Matthew Meyerson, Jill P. Mesirov, Scott L. Pomeroy
Manuscript writing: Yoon-Jae Cho, Aviad Tsherniak, Pablo Tamayo, Sandro Santagata, Azra Ligon, Heidi Greulich, Rameen Berhoukim, Vladimir Amani, Liliana Goumnerova, Charles G. Eberhart, Ching C. Lau, James M. Olson, Richard J. Gilbertson, Amar Gajjar, Olivier Delattre, Marcel Kool, Keith Ligon, Matthew Meyerson, Jill P. Mesirov, Scott L. Pomeroy
Final approval of manuscript: Yoon-Jae Cho, Aviad Tsherniak, Pablo Tamayo, Sandro Santagata, Azra Ligon, Heidi Greulich, Rameen Berhoukim, Vladimir Amani, Liliana Goumnerova, Charles G. Eberhart, Ching C. Lau, James M. Olson, Richard J. Gilbertson, Amar Gajjar, Olivier Delattre, Marcel Kool, Keith Ligon, Matthew Meyerson, Jill P. Mesirov, Scott L. Pomeroy

REFERENCES

1. Pomeroy SL, Tamayo P, Gaasenbeek M, et al: Prediction of central nervous system embryonal tumour outcome based on gene expression. Nature 415:436-442, 2002

2. Brunet JP, Tamayo P, Golub TR, et al: Metagenes and molecular pattern discovery using matrix factorization. Proc Natl Acad Sci U S A 101:4164-4169, 2004

3. Kool M, Koster J, Bunt J, et al: Integrated genomics identifies five medulloblastoma subtypes with distinct genetic profiles, pathway signatures and clinicopathological features. PLoS One 3:e3088, 2008

4. Thompson MC, Fuller C, Hogg TL, et al: Genomics identifies medulloblastoma subgroups that are enriched for specific genetic alterations. J Clin Oncol 24:1924-1931, 2006

5. Kim JY, Nelson AL, Algon SA, et al: Medulloblastoma tumorigenesis diverges from cerebellar granule cell differentiation in patched heterozygous mice. Dev Biol 263:50-66, 2003

6. Clifford SC, Lusher ME, Lindsey JC, et al: Wnt/Wingless pathway activation and chromosome 6 loss characterize a distinct molecular sub-group of medulloblastomas associated with a favorable prognosis. Cell Cycle 5:2666-2670, 2006

7. Fattet S, Haberler C, Legoix P, et al: Beta-catenin status in paediatric medulloblastomas: Correlation of immunohistochemical expression with mutational status, genetic profiles, and clinical characteristics. J Pathol 218:86-94, 2009

8. Lo KC, Rossi MR, Eberhart CG, et al: Genome wide copy number abnormalities in pediatric medulloblastomas as assessed by array comparative genome hybridization. Brain Pathol 17:282-296, 2007

9. Lo KC, Rossi MR, Burkhardt T, et al: Overlay analysis of the oligonucleotide array gene expression profiles and copy number abnormalities as determined by array comparative genomic hybridization in medulloblastomas. Genes Chromosomes Cancer 46:53-66, 2007

10. Northcott PA, Nakahara Y, Wu X, et al: Multiple recurrent genetic events converge on control of histone lysine methylation in medulloblastoma. Nat Genet 41:465-472, 2009

11. Ferretti E, De Smaele E, Po A, et al: MicroRNA profiling in human medulloblastoma. Int J Cancer 124:568-577, 2009

12. Ferretti E, De Smaele E, Miele E, et al: Concerted microRNA control of Hedgehog signalling in cerebellar neuronal progenitor and tumour cells. Embo J 27:2616-2627, 2008

13. Uziel T, Karginov FV, Xie S, et al: The miR-17~92 cluster collaborates with the Sonic Hedgehog pathway in medulloblastoma. Proc Natl Acad Sci U S A 106:2812-2817, 2009

14. Northcott PA, Fernandez-L A, Hagan JP, et al: The miR-17/92 polycistron is up-regulated in sonic hedgehog-driven medulloblastomas and induced by N-myc in sonic hedgehog-treated cerebellar neural precursors. Cancer Res 69:3249-3255, 2009

14b. Tamayo P, Cho Y-J, Tsherniak A, et al: Predicting relapse in patients with medulloblastoma by integrating evidence from clinical and genomic features. J Clin Oncol (in press)

15. Lu J, Getz G, Miska EA, et al: MicroRNA expression profiles classify human cancers. Nature 435:834-838, 2005

16. Lu Y, Ryan SL, Elliott DJ, et al: Amplification and overexpression of Hsa-miR-30b, Hsa-miR-30d and KHDRBS3 at 8q24.22-q24.23 in medulloblastoma. PLoS One 4:e6159, 2009

17. Rousseeuw PJ: Silhouettes: A graphical aid to the interpretation and validation of cluster analysis J Comput Appl Math 20:12, 1987

18. Verhaak RG, Hoadley KA, Purdom E, et al: Integrated genomic analysis identifies clinically relevant subtypes of glioblastoma characterized by abnormalities in PDGFRA, IDH1, EGFR, and NF1. Cancer Cell 17:98-110

19. Subramanian A, Tamayo P, Mootha VK, et al: Gene set enrichment analysis: A knowledge-based approach for interpreting genome-wide expression profiles. Proc Natl Acad Sci U S A 102:15545-15550, 2005

20. Barbie DA, Tamayo P, Boehm JS, et al: Systematic RNA interference reveals that oncogenic KRAS-driven cancers require TBK1. Nature 462:108-112, 2009

21. Beroukhim R, Getz G, Nghiemphu L, et al: Assessing the significance of chromosomal aberrations in cancer: Methodology and application to glioma. Proc Natl Acad Sci U S A 104:20007-20012, 2007

22. Beroukhim R, Mermel CH, Porter D, et al: The landscape of somatic copy number alterations across multiple human cancers. Nature 463:899-905, 2010

23. Tamayo P, Scanfeld D, Ebert BL, et al: Metagene projection for cross-platform, cross-species characterization of global transcriptional states. Proc Natl Acad Sci U S A 104:5959-5964, 2007

24. Santagata S, Maire CL, Idbaih A, et al: CRX is a diagnostic marker of retinal and pineal lineage tumors. PLoS One 4:e7932, 2009

25. Firestein R, Bass AJ, Kim SY, et al: CDK8 is a colorectal cancer oncogene that regulates beta-catenin activity. Nature 455:547-551, 2008

26. Boon K, Eberhart CG, Riggins GJ: Genomic amplification of orthodenticle homologue 2 in medulloblastomas. Cancer Res 65:703-707, 2005

27. Ellison DW, Onilude OE, Lindsey JC, et al: Beta-catenin status predicts a favorable outcome in childhood medulloblastoma: The United Kingdom Children's Cancer Study Group Brain Tumour Committee. J Clin Oncol 23:7951-7957, 2005

28. Chan JA, Krichevsky AM, Kosik KS: MicroRNA-21 is an antiapoptotic factor in human glioblastoma cells. Cancer Res 65:6029-6033, 2005

29. Central Brain Tumor Registry of the United States: Statistical Report: Primary Brain and Central Nervous System Tumors Diagnosed in the United States in 2004-2005. Central Brain Tumor Registry of the United States, Hinsdale, IL, 2009

30. Louis DN, Ohgaki H, Wiestler OD, et al: The 2007 WHO classification of tumours of the central nervous system. Acta Neuropathol 114:97-109, 2007

31. Loscher CJ, Hokamp K, Kenna PF, et al: Altered retinal microRNA expression profile in a mouse model of retinitis pigmentosa. Genome Biol 8:R248, 2007

32. Loscher CJ, Hokamp K, Wilson JH, et al: A common microRNA signature in mouse models of retinal degeneration. Exp Eye Res 87:529-534, 2008

33. Viswanathan SR, Mermel CH, Lu J, et al: MicroRNA expression during trophectoderm specification. PLoS One 4:e6143, 2009

34. Romer JT, Kimura H, Magdaleno S, et al: Suppression of the SHH pathway using a small molecule inhibitor eliminates medulloblastoma in Ptc1(+/-)p53(-/-) mice. Cancer Cell 6:229-240, 2004

35. Sasai K, Romer JT, Lee Y, et al: SHH pathway activity is down-regulated in cultured medulloblastoma cells: Implications for preclinical studies. Cancer Res 66:4215-4222, 2006

